Printed in the Republic of Korea

ANALYTICAL SCIENCE & TECHNOLOGY

Vol. 38 No. 5, 314-332, 2025

https://doi.org/10.5806/AST.2025.38.5.314

QbD-based stability-indicating UPLC method for the analysis of fruquintinib and its impurities with MS/MS characterization of degradation products

K.V. Umamaheswara Rao[1], Dhanashree K Keny[1], and Neetu Shorgar[2,★]

[1]*Research Scholar, Department of Chemistry, Faculty of Science, Pacific Academy of Higher Education and Research University, Udaipur-313001, Rajasthan*

[2]*Professor and Head of Department, Department of Chemistry, Faculty of Science, Pacific Academy of Higher Education and Research University, Udaipur-313001, Rajasthan*

(Received January 6, 2025; Revised March 6, 2025; Accepted April 11, 2025)

Abstract: A strong and selective analytical technique was also created for the simultaneous determination of fruquintinib along with its impurities through a Quality by Design (QbD) strategy. UV spectral characterization of the compounds determined 265 nm as the iso-absorptive wavelength for both fruquintinib and the impurities. Chromatographic separation was conducted on a BEH C18 column with a mobile phase consisting of 5 mM ammonium formate (pH 3.5), acetonitrile, and methanol (45:35:20, v/v) at 0.3 mL/min flow rate under isocratic conditions. Optimization using DoE indicated that mobile phase pH was the prime factor for separating closely eluting impurities. The method showed excellent specificity, linearity ($R^2 > 0.999$), precision (%RSD < 0.74 %), accuracy (98–102 %), and sensitivity (LOD = 0.075 µg/mL). Forced degradation studies established extensive degradation under acidic hydrolysis (81.02 % assay remaining), six DPs (Degradation products) being formed. Oxidative stress resulted in moderate degradation (14.25 %) with three major DPs, whereas alkaline and reductive conditions resulted in degradation of <4 %. In peroxide degradation, DP5 (*m*/z 223.1976) was detected as 6,7-*dimethoxyquinazolin-4-yl hydroperoxide*, which with oxidative demethylation gave DP2 (*m*/z 195.1444). Acid hydrolysis gave DP8 (*m*/z 381.3506) through *N-methylamide* hydrolysis, which in turn converted to DP6 (*m*/z 353.2979) and finally to DP3 (*m*/z 207.1979) and DP1 (*m*/z 177.1443) through demethylation and ether cleavage. This QbD-based procedure provides excellent stability-indicating ability and efficiently identifies important degradation products of fruquintinib under stress conditions.

Key words: impurities of fruquintinib, qbd approach, stress degradation studies, MS/MS characterization

Introduction

The development of a pharmaceutical drug involves multidisciplinary fields that require a rigorous and systematic approach to ensure the safety, efficacy, and quality of therapeutic agents. Among the wide

★ Corresponding author
Phone : 91 95504 20700
E-mail : nshorgar@gmail.com

range of pharmaceutical compounds, anti-cancer agents like fruquintinib (*Fig.* 1) hold significant clinical significance. Fruquintinib is a highly selective vascular endothelial growth factor receptor (VEGFR) inhibitor drug that was developed primarily in treating metastatic colorectal cancer and other solid tumors.[1] Its mechanism of action involves potent inhibition of VEGFR-1, VEGFR-2, VEGFR-3 and leads to anti-angiogenic effects and tumor growth suppression. It was imperative to develop robust and reliable analytical methods for its quality control and impurity profiling of fruquintinib due to its promising therapeutic profile and increase in clinical applications.[2]

In recent years, the concept of QbD has emerged as a transformative paradigm in pharmaceutical development that provides a scientific, risk-based, and proactive framework for the development of analytical methods. The application of QbD principle ensures that analytical method not only robust and reliable but also capable to deliver intended performance throughout the drug lifecycle. The QbD implementation in method development defines the Analytical Target Profile (ATP), identify Critical Method Parameters (CMPs) and Critical Quality Attributes (CQAs), conduct risk assessment and optimize method performance by employing DoE strategy.[3,4]

Fruquintinib may be susceptible to degradation under various environmental and chemical stress conditions. This degradation can lead to the formation of DPs that may possess toxicological risks and can also impact the drug's efficacy.[5] The regulatory guidelines mandate the identification and quantification of such impurities and DPs to ensure drug safety and quality. The ICH guidelines Q3A(R2) and Q3B(R2) provides the framework to identify, report and qualify impurities in drug substances and drug products.[6,7] The stability-indicating methods are thus essential to detect the changes in drug purity over time under the influence of environmental factors such as temperature, humidity, light, and oxidizing conditions.

In recent times, UPLC (Ultra Performance Liquid Chromatography) has emerged as a superior analytical tool to analyse trace quantity of pharmaceutical impurities due to its enhanced resolution, speed, and sensitivity. It utilizes smaller particle size columns that enables faster analysis and improves separation efficiency. This technique was particularly advantageous during the analysis of complex pharmaceutical formulations with multiple impurities and DPs. In parallel, LC-MS/MS (Liquid Chromatography – Tandem Mass Spectrometry) serves as a powerful analytical tool for the structural elucidation and characterization of DPs and impurities. It provides high sensitivity and specificity that enables the detection of low-level impurities and offers valuable insights into the molecular structure of DPs. The combined application of stability-indicating UPLC method with MS/MS enhances the comprehensiveness of impurity profiling and degradation studies.[8]

Despite the therapeutic significance of fruquintinib, the available literature is limited to UPLC-MS/MS[9] and HPLC-MS/MS[10] methods its quantification in rat plasma. One simultaneous quantification method reported to quantify fruquintinib along with other similar class drugs in human plasma.[11] The reported studies focused on pharmacokinetics, clinical efficacy, and quantification of fruquintinib in biological matrices. However, no QbD-based method has been reported for analysis of fruquintinib and its impurities along with LC-MS/MS characterization of DPs under forced degradation conditions. This presents a significant gap in analytical research and hence the current study aims to bridge this gap to develop a QbD-based stability-indicating UPLC method for the quantitative analysis of fruquintinib and its known impurities. The impurities 1 to 4 of fruquintinib (*Fig.* 1) was selected in this optimization study based on availability. The proposed method was further extended to identify and characterize DPs formed under ICH-recommended forced degradation conditions.

In this context, this study aims at ensure propose a robustness and reliable analytical method for quantification of Fruquintinib and its impurities. In the development process, a systematic QbD approach was employed by clearly defining the ATP, identify CMPs and CQAs, and apply DoE. Fruquintinib was subjected to series of forced degradation studies to evaluate its intrinsic stability under various stress

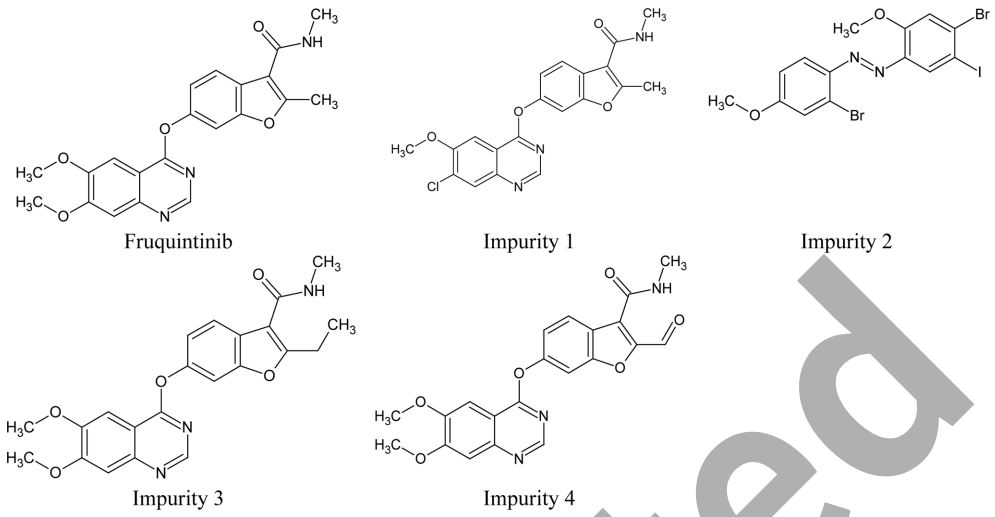

Fig. 1. Molecular structure of fruquintinib and its known impurities selected in this study.

conditions. The DPs formed were characterized using LC-MS/MS, with structural elucidation based on MS/MS fragmentation patterns, molecular ion peaks, and supportive literature data. Furthermore, the identified DPs were assessed for their potential toxicological relevance to ensure the overall safety and quality of the drug product.

2. Experimental

2.1. Materials

The main drug substance, fruquintinib with 98.75 % purity, along with its impurity 1 to 4 were generously supplied as complimentary samples by Takeda Pharmaceuticals India Private Limited, Gurugram, Haryana. All chromatographic studies were carried out using HPLC grade solvents and other chemicals of analytical reagent grade were obtained from Merck, Mumbai. The formulation assay was conducted using marketed formulation capsule of Elunate brand with 5 mg dosage and were obtained from SS Medex, Nagpur, Maharashtra.

2.2. Instrumentation and chromatographic conditions

The Acquity UPLC (Waters, MA, USA) setup coupled with a Synapt G2 Q-ToF mass spectrometer and a PDA detector, was employed for LC-MS and MS/MS analysis was used for all chromatographic experiments. This system was operated under isocratic conditions through a binary pump for effective solvent delivery. An automatic injector was connected to introduce the samples and detection was done using both UV and mass spectrometry detectors. The data collection and analysis were performed through MassLynx version 4.1 software. A precision weighing balance (Denver SI-234, Bohemia), digital pH meter (Systronics, India), an ultrasonic bath sonicator (GT Sonic, India) and borosilicate glass vacuum filtration unit (Borosil®, India) were utilized during this study.

The chromatographic resolution of fruquintinib and its impurities 1 to 4 was achieved on BEH C18 column (100 mm × 2.1 mm, 1.7 µm particle size). An isocratic elution mode was employed using mobile phase of 5 mM ammonium formate/formic acid buffer at pH 3.5, acetonitrile and methanol in 45:35:20 (v/v) at 0.3 mL/min with the column oven temperature set to 35 °C, the sample volume of 2 µL and 265 nm UV detector wavelength was confirmed for routine analysis of fruquintinib and its impurities. An equal volume mixture of acetonitrile and methanol was utilized as diluent for preparation of samples and standards.

The mass spectrometric detection and structural

characterization of DPs was performed through LC-MS which was operated in positive electrospray ionization (ESI+) mode. The source parameters optimized as 3.5 kV of capillary voltage, 150 °C of source temperature, 500 °C of desolvation temperature, 800 L/h of desolvation gas flow and cone gas flow of 50 L/h. The Argon gas was utilized as collision gas for fragmentation in product ion and MRM scan modes and these conditions enables sensitive and selective detection of fruquintinib and its DPs.

2.3. Preparation of solutions

The standard solution of fruquintinib was prepared by exactly weighing 25 mg of the standard and transferred into a 10 mL volumetric flask. The substance was dissolved in 15 mL diluent in 25 mL calibrated flask. The solution was thoroughly mixed and the final volume was made up to 25 mL with the same diluent to obtain a stock solution with a concentration of 1000 µg/mL (1 mg/mL). A series of dilutions were prepared from this primary solution to achieve calibration standards in the concentration range of 25 to 150 µg/mL. Likewise, separate stock solutions of impurities 1 to 4 were individually prepared using the same diluent to reach concentrations in 0.25 to 1.50 µg/mL range.

2.4. Method development

The method development for the analysis of fruquintinib and its impurities was undertaken with an objective to establish a reliable and reproducible UPLC method that was compatible with LC-MS/MS for further characterization of DPs.[12,13] A stepwise approach that involves the systematic variation of chromatographic conditions was adopted to identify optimal parameters that produce efficient separation, appropriate peak shapes with minimal run time. The detection wavelength for monitoring of analytes was initially selected based on UV absorption maxima of fruquintinib and its impurities. The iso-absorption wavelength of analytes was confirmed as ideal wavelength in the study.

The method optimization process began with the evaluation of different reversed-phase UPLC columns that include C18 and phenyl-hexyl columns from different manufacturers. The chromatographic result in each column change was assessed to identify the most suitable column that ensures adequate retention and resolution of fruquintinib and its impurities. The mobile phase optimization was carried by testing various combinations of aqueous and organic solvents. The aqueous component was varied between water, ammonium acetate buffer, and formic acid in water at different concentrations whereas methanol and acetonitrile were tested as organic phase. The pH of the aqueous phase was in the pH range of 3.0 to 5.5 to study the effect of ionization on retention behavior and peak shape. The flow rate was varied from 0.2 to 0.5 mL/min to evaluate its impact on resolution and analysis time. Additionally, the column temperature was optimized in between 25 °C and 45 °C to study its influence on retention and sharpness of peaks.[14]

2.5. QbD-based optimization strategy

The QbD approach was employed in the final phase of optimization to ensure robustness and reliability method. This systematic methodology enables the identification and control of critical method parameters (CMPs) that significantly influence the chromatographic performance of fruquintinib and its impurities. The pH of the mobile phase was recognized as critical method parameter (CMP) due to its substantial impact on the ionization state of analytes, retention behavior, and resolution. The DoE approach was applied to study the effect of pH on chromatographic parameters of fruquintinib and its impurities. These experimental data were organized and interpreted through Design Expert® software (Version 11.0, Stat-Ease Inc.). Further, the risk assessment was performed as per ICH Q8 and Q9 to ensure the method reliability. This involves the evaluation of method performs when small changes are made to operating conditions or the analysis was performed by different analysts.

2.6. Method validation

The reliability of method for routine use was assessed by performing method validation studies and was conducted in accordance with ICH Q2 (R2) guidelines.[15]

The method specificity was established by evaluating the ability of the method to distinctly identify fruquintinib and its impurities in the presence of DPs and excipients. The linearity range was evaluated across various concentration ranges and concentration vs area response was plotted for each analyte. The linear response graph with correlation coefficient (r^2) of not less than 0.999 was treated as acceptable range for the analysis. Accuracy was confirmed through recovery studies at three levels, with acceptance criteria set at 98–102 % recovery whereas precision was determined by calculating the %RSD of peak area responses, which should not exceed 2.0 % for both intra-day and inter-day analyses. Method sensitivity in terms of LOD and LOQ was derived based on the standard deviation of y-intercept and slope of the calibration curve. Robustness was evaluated by introducing minor deliberate changes in chromatographic conditions and must ensure that the method remained unaffected by these deliberate changes. The chromatographic results such as retention time, theoretical plate count (not less than 2000), tailing factor (not more than 2.0), and %RSD for replicate injections (not more than 1.0 %) confirms the method system suitability.

2.7. Forced degradation studies

Forced degradation experiments were conducted as per ICH guidelines[16] to assess the chemical stability of fruquintinib when exposed to different stress conditions. In acidic stress, 25 mg of fruquintinib was weighed and placed in a 25 mL volumetric flask and was treated with 1 mL of hydrochloric acid (1 N) solution and then kept aside for 15 min to induce degradation. Then, the solution was neutralized using sodium hydroxide (1 N) solution and made up to volume with the prepared diluent. Similarly, in alkaline degradation, the same procedure was followed by adding 1 mL of 1N sodium hydroxide and was later neutralized with 1 N hydrochloric acid. In oxidative stress, 25 mg of drug was mixed with 1 mL of 10 % hydrogen peroxide and allowed to react for 15 min. The reductive degradation was carried through 1 mL of 10 % sodium bisulfite solution under the same time conditions. In thermal degradation, 25 mg of fruquintinib was placed in an oven at 105 °C for six hours and then the sample was dissolved in 7 mL of diluent. The content was sonicated for 5 min and then filtered prior to analysis. In the case of photolytic degradation, 25 mg of the drug was exposed to a photostability chamber for six hours whereas the drug was treated with 1 mL of HPLC-grade water for 15 min followed by sonication, dilution, and filtration in hydrolytic degradation. All treated samples were analysed using the developed UPLC method to detect DPs and confirms method specificity.

3. Results and Discussion

3.1. Optimization of chromatographic conditions using DoE

The method development for the simultaneous estimation of fruquintinib and its related impurities was initiated by identifying appropriate detection wavelength. The UV spectral scan confirms an isosbestic point wavelength of 265 nm as common suitable wavelength for the detection of fruquintinib and four known impurities and therefore, this wavelength was selected and employed throughout the optimization.

The initial chromatographic condition was performed using an ACQUITY BEH Phenyl column (100 mm) with mobile phase consists of an equal proportion of ammonium formate buffer and methanol in a 50:50 (v/v) ratio at 0.3 mL/min. In these conditions, the separation of analytes was unsatisfactory, as no significant resolution was observed between fruquintinib and its impurities. This result indicates that the phenyl stationary phase was not effective to discriminate these compounds (*Fig.* 2A). Further Phenyl-Hexyl column (100 mm) was utilized to enhance separation while rest of the chromatographic parameters were unchanged. However, the resultant chromatogram shows only three peaks, corresponding to the fruquintinib and two impurities. This result suggests that an incomplete resolution and co-elution of some impurities occurred in this column demonstrate that the phenyl-hexyl stationary phase also lack the selectivity requires for complete separation of all

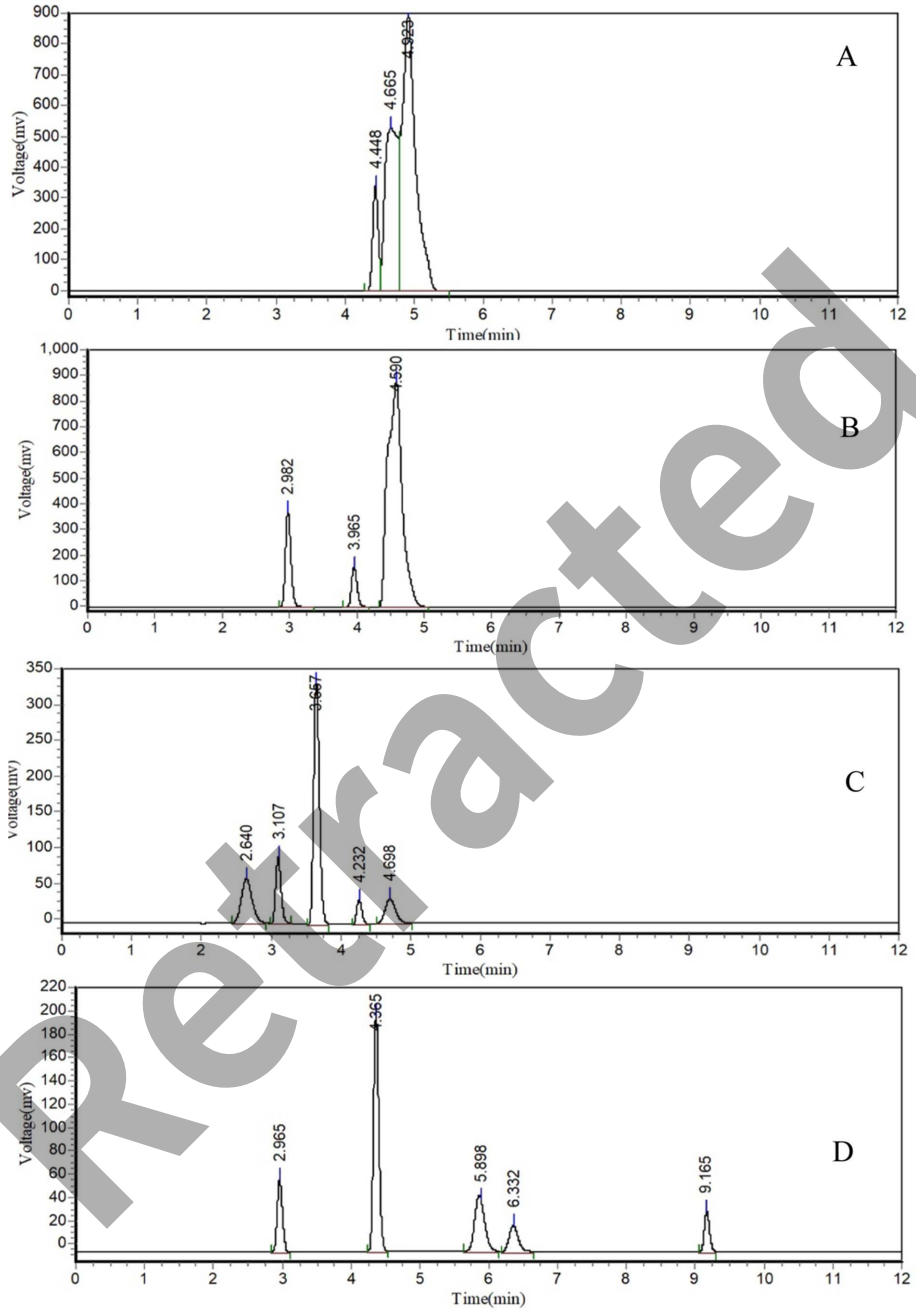

Fig. 2. Chromatograms noticed (A) Trail 1, (B) Trail 2, (C) Trail 3, (D) Trail 4 during the optimization of analytical method for the analysis of fruquintinib and its impurities.

analytes (*Fig.* 2B).

The optimization was further conducted using a BEH C18 (100 mm) column to improve the separation performance. This column shows noticeable improvement in separation and the peaks corresponds to all analytes in the study were detected. However, the resolution between the peaks was still suboptimal suggest the modification in mobile phase components.

In this, broad and asymmetrical peaks were observed for impurities 2 and 4 with relatively low peak area responses suggest that this condition was unsuitable for accurate quantification (*Fig.* 2C).

In order to overcome these limitations, further optimization was pursued by retaining the BEH C18 column and modify the mobile phase composition. A new mobile phase system was prepared using a buffer of 5 mM ammonium formate adjusted to pH 4.0 with formic acid, and a combination of methanol and acetonitrile as organic modifiers. This mobile phase significantly improved the peak shape, symmetry, and resolution of all analytes. The incorporation of both methanol and acetonitrile offers complementary selectivity, enhance separation through differing elution strengths and solvent polarity (*Fig.* 2D).

Further optimization indicated that the mobile phase pH plays a critical role to affect the ionization state of fruquintinib and its impurities. Hence, fine-tune the buffer pH was undertaken using a QbD approach which is a systematic risk-based strategy to evaluate the influence of mobile phase pH on analyte resolution, peak symmetry, and retention.

The QbD approach was strategically employed to optimize the chromatographic conditions for separation of impurity 3 and impurity 1 of Fruquintinib through Design-Expert® software. In this, statistically evaluate and model the impact of critical method parameters such as buffer strength and pH on resolution of impurity 3 and 1. A comprehensive contour plot (*Fig.* 3A) analysis reveals that the resolution between the two impurities was highly sensitive to variations in both pH and buffer concentration, with values rang from a low of 1.22 (indicates poor separation) to a high of 3.91 (indicates optimal separation). Among the two parameters, pH emerges as the most influential factor that significantly alters the ionization states of fruquintinib impurities and thereby enhances their differential interaction with the stationary phase and ultimately improves separation. The highest resolution was observed in high pH regions and with low buffer strength.

The 3D surface plots (*Fig.* 3B) further validate this results and exhibit pronounced curvature along the pH and clear gradient of improvement in resolution was observed with the increase of pH. These findings underscore the importance of higher pH levels within the defined design space to ensure consistent and reliable separation of impurities. Moreover, the interaction plots (*Fig.* 3C) reveal a significant interaction between pH and buffer strength in which resolution was not only influenced by each factor independently and also their combined levels. The slight decrease in resolution was noticed with the increase of buffer strength and decrease of pH whereas the increase in buffer strength and high pH enhances the resolution. This crossover interaction confirms that both these parameters must be optimized simultaneously to exploit their synergistic effects on chromatographic performance. Additionally, the one-factor plot (*Fig.* 3D) emphasizes that pH (factor B) is involved in a statistically significant interaction (AB), further reinforces the necessity of multidimensional optimization.

The Box-Cox plot for power transformations was utilized to verify the assumptions of normality and constant variance in the response data observed for resolution between impurity 3 and 1. The plot (*Fig.* 3E) reveals that the current transformation applied as "None", with a Lambda value of 1 (in blue) and best possible transformation was indicated at Lambda = 3 (in green). However, since the optimal Lambda was near the confidence boundary and the recommended transformation remains "None", suggest that this model was deemed statistically adequate without requiring any data transformation. This confirms that the residuals were sufficiently normally distributed and homoscedastic that meets the essential assumptions for analysis of variance.

Further validation of model adequacy was assessed by Normal Plot of Residuals that show residuals align closely to diagonal reference line (*Fig.* 3F). This alignment indicates that the externally student zed residuals follow a normal distribution, with no significant outliers or curvature detected. The color-coded residuals, represents different resolution values, were evenly spread around the mean, suggests that the model did not exhibit bias and that prediction

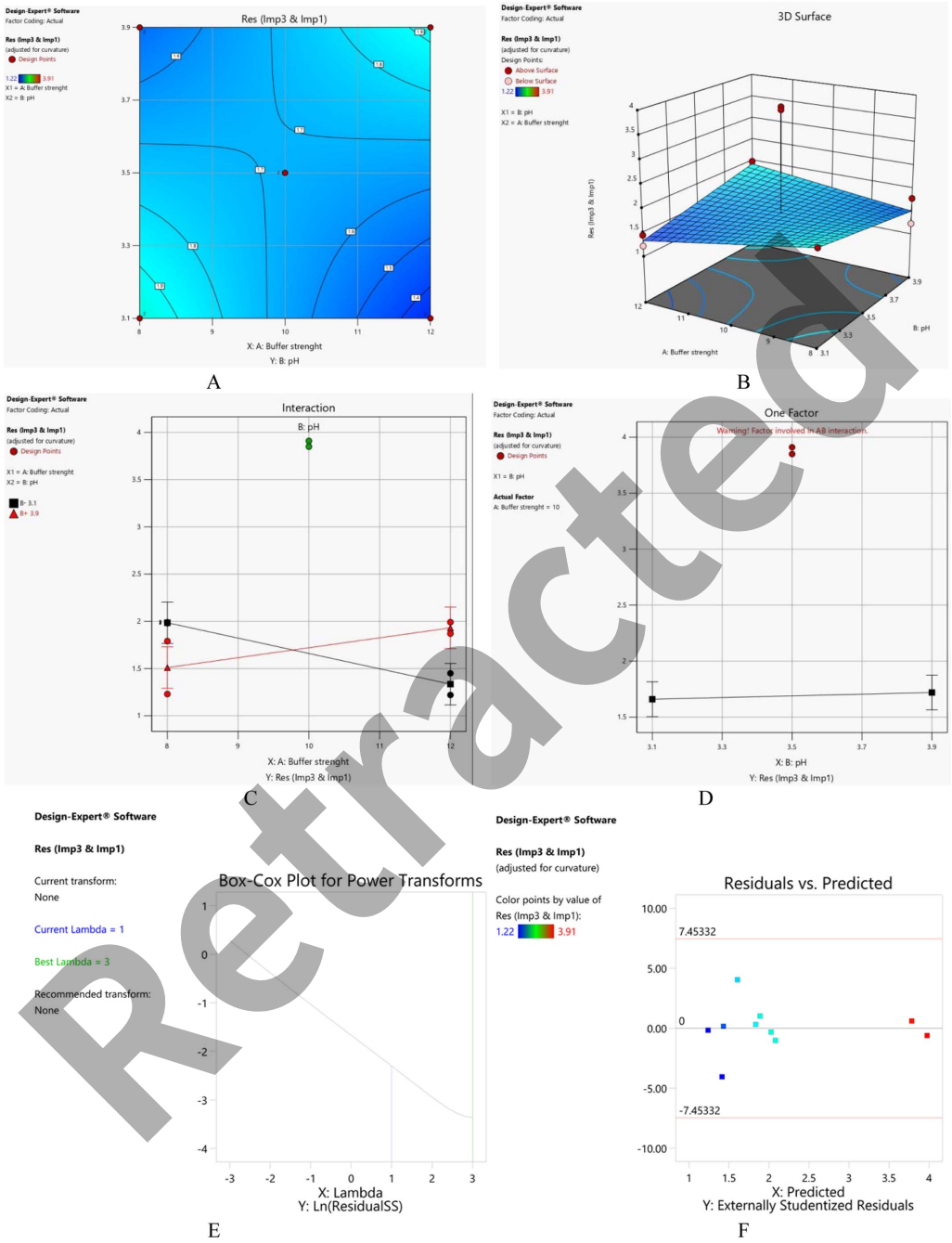

Fig. 3. Plots observed (A) contour plot (B) 3D surface plots (C) interaction plots (D) one-factor plot (E) Box-Cox plot (F) Normal Plot as standard outputs in DoE using Design-Expert® software under a QbD framework during the method optimization for the analysis of fruquintinib and its impurities.

errors were randomly distributed. These results confirm that the optimized chromatographic method is not only analytically sound but also statistically robust and requires no further transformation or adjustments. Hence, the developed method can be confidently employed for routine impurity profiling

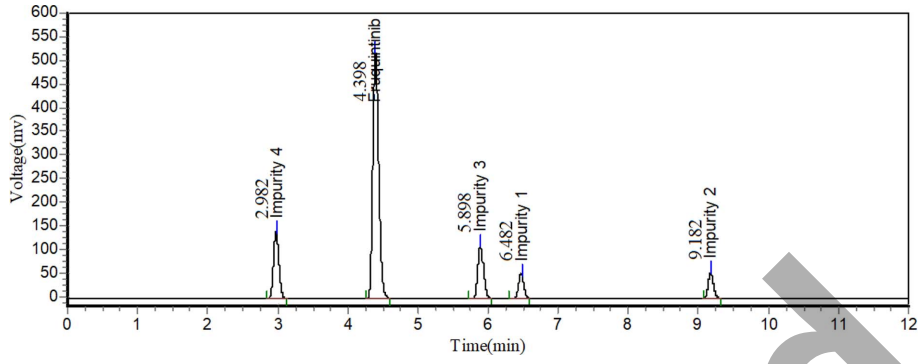

Fig. 4. Chromatogram observed in the optimized conditions for the analysis of fruquintinib and its impurities.

and quality assurance of fruquintinib in pharmaceutical formulations.

The results obtained from the QbD based DoE approach were instrumental to finalize the optimized chromatographic conditions for the effective analysis of fruquintinib and its impurities. The chromatographic separation was successfully achieved with high resolution and efficiency on BEH C18 (100 mm × 2.1 mm and 1.7 µm particle size) that was set at 35 °C. An isocratic elution technique was selected for its simplicity and consistency by utilizing mobile phase consisting of 5 mM ammonium formate/formic acid buffer (adjusted to pH 3.5), acetonitrile, and methanol in 45:35:20 (v/v) at 0.3 mL/min. A small injection volume of 2 µL and UV detector at 265 nm was found to be optimal for analysis of fruquintinib and its impurities with enhanced peak resolution. This QbD-driven method development strategy led to a thoroughly optimized chromatographic method that was suitable for the routine quality control and impurity profiling of fruquintinib in pharmaceutical formulations. The representative chromatogram observed in the finalized method conditions was presented in *Fig.* 4.

3.2. Validation of proposed method

The standard solution analysis using this proposed method demonstrates its effectiveness to achieve well-separated, symmetrical, and consistent peaks for Fruquintinib and its impurities. In specificity study, no peaks were detected in the chromatograms confirm that there was no interference from blank or placebo solutions. This indicates that the method is highly selective for fruquintinib and its impurities with no signal overlaps from excipients or formulation components. The USP tailing factor for fruquintinib and its impurities in range of 0.96 to 1.08 suggests that the method produce good peak symmetry with minimal distortion. The plate counts that reflect the column efficiency was noticed to be higher than the acceptable level indicates the satisfactory separation performance of method. Furthermore, all USP resolution values were above the acceptable limits, confirms clear separation between all analytes. The observed specificity results along with other chromatographic performance metrics support the method suitability. Linearity was evaluated by preparing and analysing calibration standards across a wide concentration range. The method shows an excellent linear relationship between analyte concentration and peak response between 25–150 µg/mL for fruquintinib and 0.25–1.5 µg/mL for impurities. The correlation coefficient (R^2) for all analytes was greater than 0.999 indicate strong linearity. This result confirms that the method was reliable and accurate to quantify fruquintinib and its impurities over the studied concentration ranges.

In precision study, the %RSD of 0.23 % was noticed for fruquintinib whereas the impurities in the range of 0.30 % to 0.59 %. These results were well within acceptable limits suggests that the method provides consistent and reproducible results. In intermediate precision also produce similar outcomes with %RSD of 0.30 % for fruquintinib and impurities in the range of 0.32 % to 0.74 %. The permissible %

Table 1. Validation summary results noticed for the method proposed for the analysis of fruquintinib and its impurities

Parameter	Results noticed for				
	Fruquintinib	Impurity 1	Impurity 2	Impurity 3	Impurity 4
Linearity					
Range (µg/mL)	25 – 150	0.25 – 1.50	0.25 – 1.50	0.25 – 1.50	0.25 – 1.50
Intercept	795.3	753.2	1142.8	1115.8	795.3
Slope	58765.3	53700.4	70261.9	78432.9	58765.3
Correlation (r^2)	0.9997	0.9996	0.9995	0.9996	0.9997
Precision[$$]					
Within same day	0.23	0.35	0.59	0.30	0.57
Within 3 days	0.30	0.44	0.74	0.61	0.32
Ruggedness	0.26	0.09	0.10	0.26	0.41
LOQ range	--	0.56	0.08	0.54	0.73
50 % accuracy[$]					
Prepared (µg/mL)	75	0.75	0.75	0.75	0.75
Recovered (µg/mL)	74.69	0.74	0.75	0.76	0.74
% Recovery	99.58	98.58	100.28	100.79	98.93
100 % accuracy[$]					
Prepared (µg/mL)	100	1	1	1	1
Recovered (µg/mL)	98.79	0.99	0.99	1.00	1.00
% Recovery	98.79	99.01	99.36	99.58	100.25
150 % accuracy[$]					
Prepared (µg/mL)	125	1.25	1.25	1.25	1.25
Recovered (µg/mL)	123.41	1.26	1.26	1.24	1.24
% Recovery	98.73	100.58	100.67	99.47	99.31

n=3 ($) and n = 6 ($$)

RSD results noticed for all the impurities at LOQ level again confirms the method's reliability. Accuracy was evaluated through recovery studies at three levels in and %RSD values in each level was less than 1 %. The % recovery of fruquintinib and its impurities shows with in desired level of 98 to 102 % confirms the method accuracy and its consistency to recover known amounts of fruquintinib and its impurities. The method sensitivity was assessed by determining the LOD and LOQ of impurities. The LOD of 0.075 µg/mL was noticed for the impurities indicates the method can reliably detect the impurities up to this lowest concentration. This low detection values demonstrate the method possess the enough suitability suitable to detect impurities even small amounts during stability studies and impurity profiling. *Table* 1 summarize the method validation study results noticed for fruquintinib and its impurities in the proposed method.

3.3. Stress studies and characterization of DPs

The forced degradation studies were conducted under various stress conditions to evaluate the stability and identify potential degradation pathways of fruquintinib. In acidic conditions, fruquintinib exhibits significant degradation with an assay value of 81.02 % with degradation of 18.98 % degradation confirms that the drug was susceptible to acid hydrolysis. This study chromatogram display well resolved and unknown peaks correspond to DPs at elution time of 1.7 min, 2.1 min, 2.7 min, 4.7 min, 4.9 min and 7.7 min (*Fig.* 5A). In contrast, alkaline and reductive conditions demonstrate very minimal degradation with % assay of 97.69 % and 97.64 %, respectively. Notably, no DPs were observed in these chromatograms indicate that the degradation was limited and did not lead to the formation of detectable DPs. The expose to fruquintinib to oxidative stress

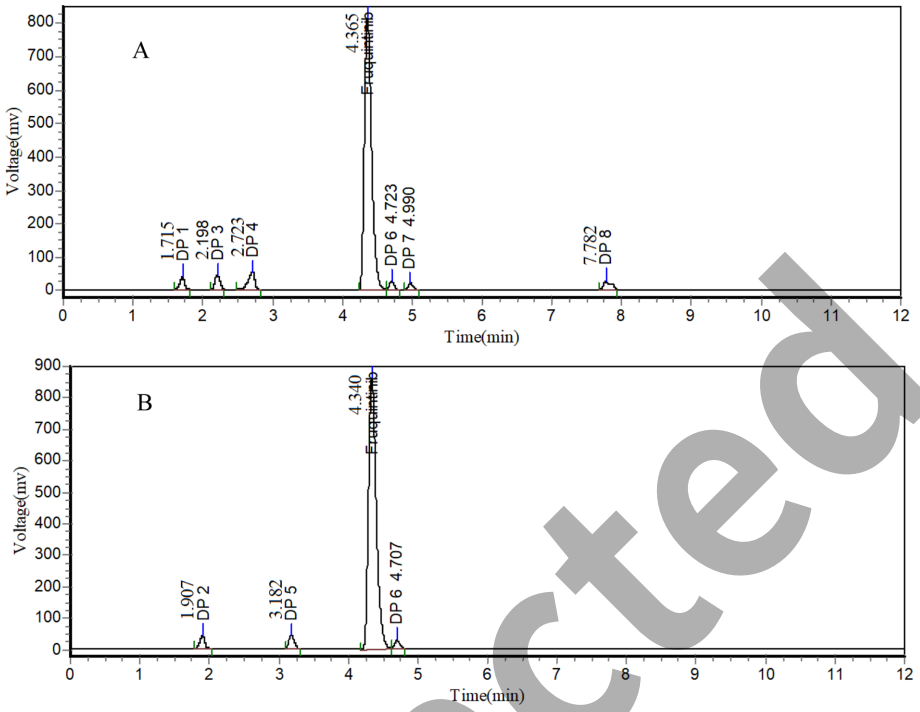

Fig. 5. Acid (A) and (B) peroxide degradation chromatograms of fruquintinib clearly shows well resolved peaks corresponds to DPs.

Table 2. Forced degradation test results observed for fruquintinib in the study

Condition	% assay	% degradation	% Mass balance	Remark
Acid	81.02	18.98	100.21	6 DPs were resolved and identified
Alkali	97.69	2.31	97.69	No DP identified
Peroxide	85.75	14.25	99.85	3 DPs were resolved and identified
Reduction	97.64	2.36	97.64	No DP identified
Photolytic	96.42	3.58	96.42	No DP identified
Hydrolysis	96.99	3.01	96.99	No DP identified
Thermal	97.45	2.55	97.45	No DP identified

using peroxide led to moderate degradation of 14.25 % with % assay value of 85.75 %. In this case, three DPs were observed confirm the susceptibility of fruquintinib towards oxidative degradation. These DPs were identified at 1.9 min, 3.1 min and 4.7 min in the chromatogram (*Fig.* 5B). The mass balance in all these conditions remain close to 100 % supports the method's reliability in accounting for both the parent compound and its DPs. The photolytic, hydrolytic, and thermal stress conditions result in relatively minor degradation, with % assay values of 96.42 %, 96.99 %, and 97.45%, respectively with % degradation in the range of 2.55 % to 3.58% (*Table* 2). There no DP detected in these conditions suggests that fruquintinib is relatively stable under light, moisture, and heat exposure.

The DP observed at 4.7 min was commonly found in both acid and peroxide stress study suggest that the same product was formed in both these conditions. There no correlation in the retention times of other DPs in both the conditions suggests that these DPs are unique in these conditions. All the formed DPs

were named as DP 1 to 8 based on increase in retention time of identified compounds and were further characterized through LC-MS/MS analysis.

In the chromatogram of peroxide degradation study, **DP 5** was observed at 3.18 min with a RRT (Relative Retention Time) of 0.73 in comparison to the parent compound and was LC–MS/MS analysis. This DP was arisen due to oxidative cleavage of the ether linkage present in the fruquintinib structure and this ether bond is susceptible to oxidative transformation that led to hydroperoxides (R–O–O–H) as intermediates. This oxidative process is typically initiated by electrophilic pathways of hydrogen peroxide on the electron-rich oxygen atom of the ether group that result in the formation of a hydroperoxide species. Subsequent decomposition of this unstable intermediate under stress conditions leads to C–O bond cleavage and yield smaller fragment molecules which was retained at an RRT of 0.73.

The LC–MS/MS analysis reveals $C_{10}H_{10}N_2O_4$ as molecular formula with an exact $[M+H]^+$ *m/z* of 223.1974 and was close match with observed *m/z* of 223.1976 with a mass error of 0.896 ppm. It has a calculated ring double bond (RDB) value of 7.0 indicates relatively unsaturated structure. The fragmentation pattern further supports the proposed structure and shows characteristic product ions at *m/z* 185.1689 ($C_8H_{10}NO_4$, RDB 4.5), 180.1525 ($C_8H_7N_2O_3$, RDB 6.5), 139.1436 ($C_7H_8NO_2$, RDB 4.5), 126.1050 ($C_5H_5N_2O_2$, RDB 4.5), and 111.1335 (C_6H_8NO, RDB 3.5). These fragment ions suggest sequential losses of functional groups such as hydroxyl, methoxy, or nitrogen-containing moieties. The consistent low ppm mass error values noticed in the study validate the mass accuracy results. Based on correlation all data, the compound DP 5 was characterized as *6,7-dimethoxyquinazolin-4-yl hydroperoxide*.

The DP 5 was characterized with formula $C_{10}H_{10}N_2O_4$ and its structure contains two methoxy ($-OCH_3$) groups attached to aromatic ring. These methoxy groups undergo oxidative demethylation under continues exposure to oxidative stress with peroxide reagents and led to conversion of method group into hydroxyl (–OH) groups that result in the formation of polar product as **DP 2**. This oxidative mechanism involves the abstraction of the methyl group from the methoxy substituent via a radical or electrophilic peroxide-mediated pathway and leads to the formation of hydroxyl groups. The loss of two methyl groups in DP 5 was converted to dihydroxy derivatives that leads to the formation of DP 2 with a molecular formula of $C_8H_6N_2O_4$ and a calculated $[M+H]^+$ *m/z* of 195.1442. The calculated mass data was matches with observed of *m/z* of 195.1444 with a minimal mass error of 1.025 ppm. The calculated RDB value of the compound was observed to be 7.0 that relate the aromatic and heterocyclic core structure similar to its precursor DP 5. The MS/MS fragmentation of DP 2 reveals the key product ions at *m/z* 178.1366 ($C_8H_5N_2O_3$, RDB 7.5) is likely due to the loss of a

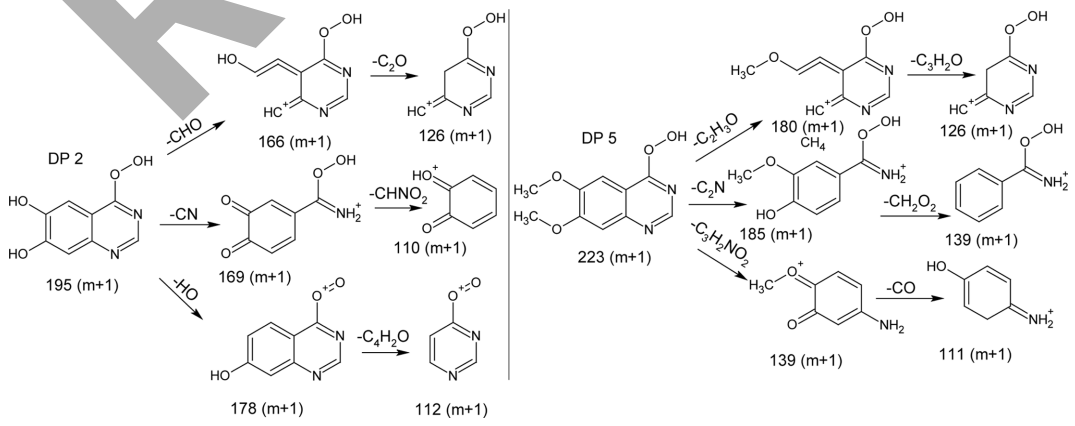

Fig. 6. Proposed fragmentation mechanism for DP 2 and 5 of fruquintinib in peroxide stress study.

Table 3. MS/MS interpretation data observed for DP 1 to 8 of fruquintinib in peroxide stress study

Name	Molecular Formula	Exact *m/z* values (m+1)	Observed *m/z* values (m+1)	Error (ppm)	RDB
Acid degradation					
	$C_8H_6N_2O_3$	179.1448	179.1445	-1.675	7.0
	$C_8H_6NO_2$	149.1381	149.1383	1.341	6.5
	$C_7H_3N_2O_2$	148.1103	148.1105	1.350	7.5
DP1	$C_7H_5N_2O$	134.1268	134.1266	-1.491	6.5
	$C_6H_5O_2$	110.1021	110.1023	1.816	4.5
	$C_4H_5N_2O$	98.0946	98.0942	-1.019	3.5
	$C_4H_3N_2$	80.0794	80.0795	1.249	4.5
	$C_{10}H_{10}N_2O_3$	207.1980	207.1979	-0.483	7.0
	$C_8H_{10}NO_3$	169.1693	169.1696	1.773	4.5
	$C_8H_7N_2O_2$	164.1528	164.1525	-1.828	6.5
DP3	$C_7H_8NO_2$	139.1433	139.1436	2.156	4.5
	$C_7H_9O_2$	126.1446	126.1449	2.378	4.0
	C_6H_8NO	111.1332	111.1334	1.800	3.5
	$C_5H_5N_2O$	110.1054	110.1052	-1.816	4.5
	$C_{11}H_{10}ClNO_2$	224.6556	224.6558	0.890	7.0
	$C_{10}H_6ClO_2$	194.6058	194.6056	-1.028	7.5
DP4	C_9H_7ClO	167.6042	167.6044	1.193	6.0
	$C_8H_5O_2$	134.1235	134.1237	1.491	6.5
	C_6H_6ClO	130.5636	130.5638	1.532	3.5
	C_6H_5O	94.1027	94.1029	2.125	4.5
	$C_{18}H_{12}N_2O_6$	353.2976	353.2979	0.849	14.0
	$C_{18}H_{11}N_2O_5$	336.2897	336.2894	-0.892	14.5
	$C_{16}H_{11}N_2O_5$	312.2683	312.2685	0.640	12.5
	$C_{15}H_{10}N_2O_4$	283.2509	283.2512	1.059	12.0
DP6	$C_{14}H_9N_2O_3$	254.2323	254.2327	1.573	11.5
	$C_{11}H_8NO_4$	219.1849	219.1852	1.369	8.5
	$C_8H_7N_2O_3$	180.1522	180.1526	2.220	6.5
	$C_8H_5N_2O_3$	178.1363	178.1368	2.807	7.5
	$C_7H_7O_3$	140.1281	140.1279	-1.427	4.5
	$C_6H_6NO_2$	125.1167	125.1164	-2.398	4.5
	$C_{19}H_{15}N_3O_5$	366.3395	366.3399	1.092	14.0
	$C_{18}H_{12}N_3O_4$	335.3050	335.3047	-0.895	14.5
	$C_{16}H_{14}N_3O_5$	329.2989	329.2986	-0.911	11.5
	$C_{17}H_{14}N_3O_4$	325.3102	325.3100	-0.615	12.5
DP7	$C_{13}H_{13}N_2O_3$	246.2533	246.2536	1.218	8.5
	$C_{11}H_9N_2O_3$	218.2002	218.2006	1.833	8.5
	$C_8H_9NO_2$	152.1625	152.1628	1.972	5.0
	$C_8H_7N_2O_3$	180.1522	180.1525	1.665	6.5
	$C_7H_8NO_2$	139.1433	139.1436	2.156	4.5
	$C_6H_6NO_2$	125.1167	125.1164	-2.398	4.5
	$C_{20}H_{16}N_2O_6$	381.3508	381.3506	-0.524	14.0
	$C_{18}H_{11}N_2O_6$	352.2891	352.2894	0.852	14.5
	$C_{19}H_{15}N_2O_4$	336.3328	336.3330	0.595	13.5
	$C_{18}H_{13}N_2O_4$	322.3062	322.3058	-1.241	13.5
DP8	$C_{12}H_{11}N_2O_3$	232.2267	232.2270	1.292	8.5
	$C_{10}H_9O_4$	194.1755	194.1759	2.060	6.5
	$C_9H_7N_2O_3$	192.1629	192.1632	1.561	7.5
	$C_9H_9N_2O$	162.1800	162.1803	1.850	6.5
	$C_7H_9O_3$	142.1440	142.1443	2.111	3.5
	$C_7H_6NO_2$	137.1274	137.1276	1.458	5.5

Table 3. Continued

Name	Molecular Formula	Exact *m/z* values (m+1)	Observed *m/z* values (m+1)	Error (ppm)	RDB
Base Degradation					
	$C_8H_6N_2O_4$	195.1442	195.1444	1.025	7.0
	$C_8H_5N_2O_3$	178.1363	178.1366	1.684	7.5
	$C_7H_6NO_4$	169.1262	169.1259	-1.774	5.5
DP2	$C_7H_5N_2O_3$	166.1256	166.1258	1.204	6.5
	$C_5H_5N_2O_2$	126.1048	126.1051	2.379	4.5
	$C_4H_3N_2O_2$	112.0782	112.0780	-1.784	4.5
	$C_6H_5O_2$	110.1021	110.1019	-1.816	4.5
	$C_{10}H_{10}N_2O_4$	223.1974	223.1976	0.896	7.0
	$C_8H_{10}NO_4$	185.1687	185.1689	1.080	4.5
DP5	$C_8H_7N_2O_3$	180.1522	180.1525	1.665	6.5
	$C_7H_8NO_2$	139.1433	139.1436	2.156	4.5
	$C_5H_5N_2O_2$	126.1048	126.1050	1.586	4.5
	C_6H_8NO	111.1332	111.1335	2.699	3.5

hydroxyl group. The fragment ion noticed at *m/z* 169.1259 ($C_7H_6NO_4$, RDB 5.5) is possibly result from cleavage of nitrogenous side chain. Further fragments noticed at *m/z* 166.1258 ($C_7H_5N_2O_3$, RDB 6.5), *m/z* 126.1051 ($C_5H_5N_2O_2$, RDB 4.5), *m/z* 112.0780 ($C_4H_3N_2O_2$, RDB 4.5) and *m/z* 110.1019 ($C_6H_5O_2$, RDB 4.5) are further confirms the proposed structure of DP 2. *Fig.* 6 presents the fragmentation mechanism of DP 2 and 5 whereas its MS/MS data summarized in *Table* 3 and mass spectra's observed for the study is given in Supplementary file from S1-S8.

In acidic degradation study, the terminal *N*-methylamide (–CO–NHCH$_3$) group of fruquintinib undergoes hydrolysis to free carboxylic acid moiety (–COOH) and was designated as **DP 8** based on retention time in the chromatogram. The mechanism involves initial protonation of the amide carbonyl oxygen, which increases the electrophilicity of the carbon atom and subsequent nucleophilic attack by water lead to tetrahedral intermediate formation. This intermediate was further bond rearrangement and expulsion of the methylamine group (CH_3NH_2) and stabilizes with the formation of free carboxylic acid moiety. This formed DP 8 was identified at 7.78 min in acid stress chromatogram with an RRT of 1.78 indicates that the molecule is relatively non-polar and elutes later in the chromatographic run due to its preserved hydrophobic aromatic structure.

LC–MS/MS suggest the molecular ion of DP 8 as *m/z* 381.3506 with formula of $C_{20}H_{16}N_2O_6$. The mass loss identified in DP 8 was in correlation with the mechanism proposed for the formation of DP 8 from fruquintinib. The exact mass of DP 8 was in close agreement with theoretical value of 381.3508 with minimal error of -0.524 ppm. The RDB of DP 8 was noticed to be 14.0 and was supported the presence of multiple unsaturated and aromatic rings in consistent with the known structure of fruquintinib. In mass spectra, major fragment ions noticed at *m/z* 352.2894 ($C_{18}H_{11}N_2O_6$) due to the loss of a small neutral fragment such as C_2H_5. The other fragments noticed at *m/z* 336.3330 ($C_{19}H_{15}N_2O_4$) and *m/z* 322.3058 ($C_{18}H_{13}N_2O_4$) due to the sequential loss of oxygen atoms through decarboxylation and deamination. The additional fragments like *m/z* 232.2270 ($C_{12}H_{11}N_2O_3$) and *m/z* 194.1759 ($C_{10}H_9O_4$) were noticed in the spectrum and were formed due to the breakdown of side chains with no breakdown in key aromatic and nitrogen-containing functionalities. Based on characterization data, DP 8 was identified as carboxylic acid derivative of fruquintinib which was formed by the conversion of *N*-methylamide group to carboxylic acid.

In acid degradation, the DP 8 was further transformed to **DP 6** via O-demethylation mechanism. Specifically,

the two methoxy (–OCH_3) groups present in the aromatic rings of DP 8 undergo hydrolytic cleavage to convert hydroxyl groups (–OH). This transformation was commonly observed in acid-catalyzed demethylation reactions observed in methoxy-substituted aromatic compounds. The mechanism involves protonation of the methoxy oxygen that enhances the electrophilicity of the methyl group and facilitates nucleophilic attack by water. The methyl group is displaced as methanol (CH_3OH) that leads to the formation of phenolic –OH functionality. The formed DP 6 was detected at 4.72 min in the chromatogram with an RRT of 1.07. This DP possess more polar nature compared to DP 8 due to the presence of two hydroxyl groups that enhance its hydrogen-bonding interactions with the stationary phase and decreases its retention time. In LC-MS analysis, the molecular ion of DP 6 was appeared at *m/z* 353.2979 corresponds to the molecular formula $C_{18}H_{12}N_2O_6$. The compound DP 6 exhibits a 28 Da (2 × 14 Da) low molecular weight than DP 8 (*m/z* 381.3506) due to the loss of two methyl groups (–CH_3). This mass difference directly supports the conversion of two –OCH_3 groups into –OH and proved that DP 6 as the dehydroxylated analogue of DP 8.

The aryl ether linkage presents in fruquintinib or the formed DP 8 undergoes acid hydrolysis in the presence of hydrochloric acid to form **DP 3**. The protonation of the ether oxygen leads to the generation of good leaving group that facilitate the cleavage of the C–O bond and formation of smaller molecular fragment that was designated as DP 3. The compound was identified at 2.198 min with an RRT of 0.503 confirm that the compound has significant increase in polarity than its precursor such as standard or DP 8 due to the introduction of hydroxyl group and the removal of hydrophobic moiety. The molecular formula of DP 3 was confirmed as $C_{10}H_{10}N_2O_3$ with an observed *m/z* of 207.1979 and a mass error of -0.483 ppm. The LC–MS/MS characterization reveals a distinct fragmentation pattern that corroborates its structural identity. The key fragment ions observed includes *m/z* 169.1696 ($C_8H_{10}NO_3$), 164.1525 ($C_8H_7N_2O_2$), *m/z* 139.1436 ($C_7H_8NO_2$), 126.1449 ($C_7H_9O_2$) and *m/z* 111.1334 (C_6H_8NO), and 110.1052 ($C_5H_5N_2O$) further suggest the proposed structure and fragmentation mechanism. The compound was characterized as *6,7-dimethoxyquinazolin-4-ol*.

The continuous acid degradation leads to the conversion two aromatic methoxy (–OCH_3) groups in DP 3 in to demethylation to form **DP 1**. This conversion of DP 3 ($C_{10}H_{10}N_2O_3$) to DP 1 ($C_8H_6N_2O_3$) involves the net loss of two methyl groups (–CH_3) and same was confirmed by mass reduction of 30 Da in the mass spectra. This mass loss is consistent with the transformation of two methoxy substituents to hydroxyl group that does not alter the oxygen count but significantly change the molecule's polarity and fragmentation behavior. This was identified at 1.715 min the chromatogram indicates increase in polarity due to the hydroxyl substitution. Its observed *m/z* value of 179.1445 and was very close to the theoretical *m/z* of 179.1448, with an error of -1.675 ppm and an RDB of 7.0. This indicates that the aromatic and heterocyclic core remains intact. The fragmentation mechanism and MS/MS data observed proved the compound as *quinazoline-4,6,7-triol*.

The two methoxy (–OCH_3) groups attached to the aromatic ring fruquintinib were susceptible to hydrolytic cleavage which is a process commonly known as acid-mediated O-demethylation. This reaction leads to the formation of phenolic –OH groups in place of the original methoxy substituents and results in the formation of **DP 7** with a retention time of 4.99 min and a RRT of 1.13. In the mass spectrum, the protonated molecular ion $[M+H]^+$ of DP 7 was observed at *m/z* 366.3399 which was very close to the theoretical value of 366.3395 with a minimal error of 1.092 ppm. The fruquintinib molecule typically shows a molecular ion at *m/z* 394.35 ($C_{21}H_{19}N_3O_5$) and its transformation in to DP 7 involves a mass loss of 28 Da that was precisely account for the loss of two methyl groups (2 × 14 Da) from the methoxy positions. This mass difference confirms the replacement of –OCH_3 with –OH. The overall RDB remains high (14) and the mass fragmentation mechanism was noticed to be very similar to standard suggest the preservation of the conjugated and aromatic system in this DP 7. The mass spectrum of DP 7 visualizes key fragment

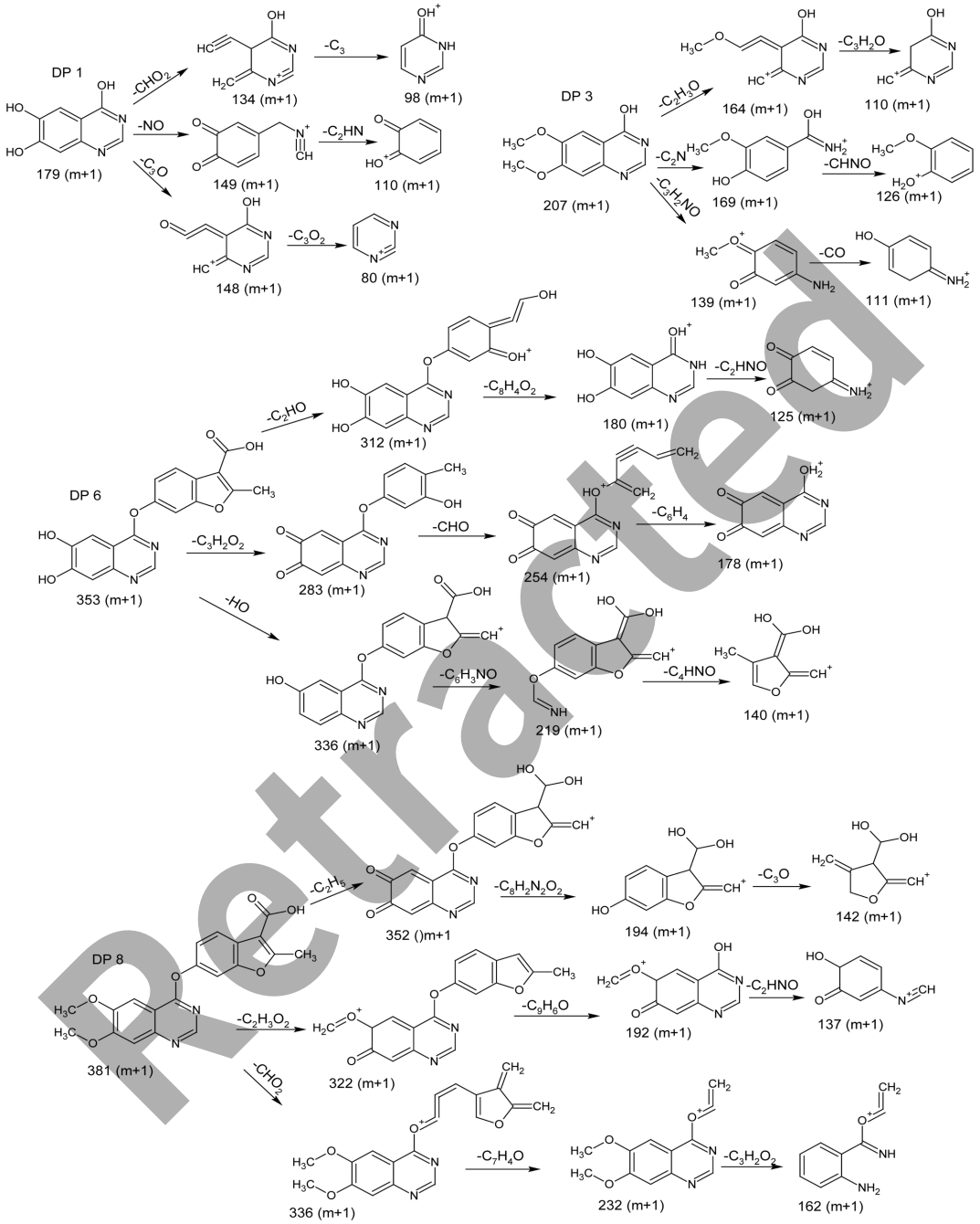

Fig. 7. Proposed fragmentation mechanism for DP 1, 3, 6 and 8 of fruquintinib in acid stress study.

ions at *m/z* 335.3047 indicates the loss of CH_2O (30 Da). The fragment at *m/z* 329.2986 suggests ring cleavage with oxygenated side chain retention whereas *m/z* 325.3100 implies a possible rearrangement or water loss from the hydroxylated intermediate. Additional Fragments ions noticed at *m/z* 246.2536, 218.2006, 180.1525 and 152.1628 further confirms the degradation pathway of DP 7. Based on correlation, it was

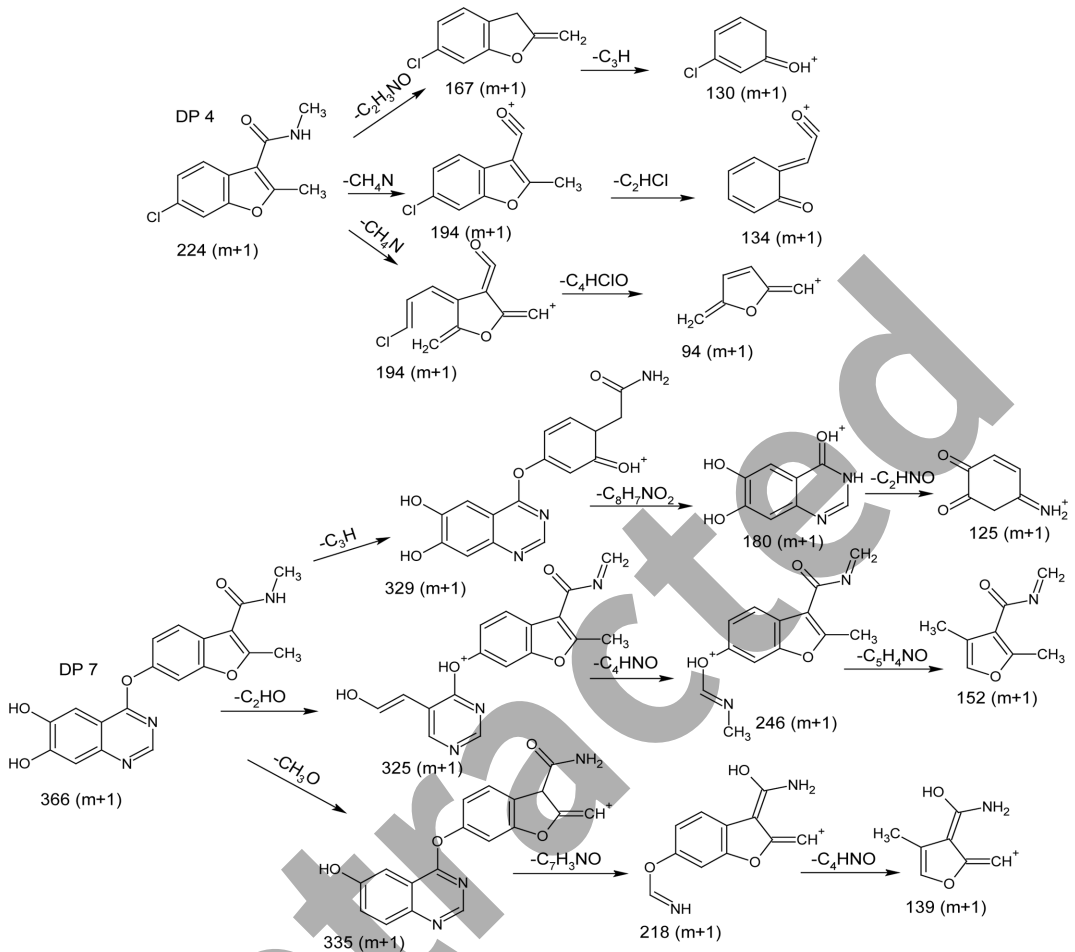

Fig. 8. Proposed fragmentation mechanism for DP 4 and 7 of fruquintinib in acid stress study.

confirmed that DP 7 is a demethylated derivative of fruquintinib that was formed under acidic stress via hydrolysis of two methoxy groups to phenols.

The prolonged acid hydrolysis leads to the breakdown of ether linkage to form in DP 7 to form R-Ar-Cl moiety and was identified as **DP 4**. The HCl utilized in acid stress study facilitate this chlorination process via electrophilic aromatic substitution and this transformation was further confirmed through LC-MS/MS. The parent ion fragment identified at *m/z* 224.6558 ($C_{11}H_{10}ClNO_2$) confirms the presence of a chlorine-substituted aromatic system. The fragment ions such as *m/z* 194.6056 ($C_{10}H_6ClO_2$) and *m/z* 167.6044 (C_9H_7ClO) support the presence of chloroarene moieties and indicates progressive loss of side chains or functional groups. The fragment at *m/z* 134.1237 ($C_8H_5O_2$), 130.5638 and 94.1029 further confirms the substitution of the aromatic ring with chlorine and loss of the original hydroxylated or methoxylated substituents seen in DP 7. This data collectively supports the structural transformation of DP 7 into a more electrophilic, chlorinated DP 4. The collective summarization of data confirms the compound as *6-chloro-N,2-dimethyl-1-benzofuran-3-carboxamide*.

4. Conclusion

This study was undertaken with the primary objective to develop a robust, accurate, and precise chroma-

tographic method for the simultaneous estimation of fruquintinib and its impurities through QbD approach. This work emphasizes a science and risk-based strategy to systematically optimize chromatographic parameters that ensure high resolution, specificity, and stability-indicating capabilities and regulatory compliance. The method development initiated with the identification of an appropriate detection wavelength and 265 nm was selected as iso-absorptive point suitable for fruquintinib and its known impurities. The initial method optimization trials using a BEH Phenyl and Phenyl-Hexyl columns failed to provide sufficient resolution among all analytes. A significant improvement was noted on BEH C18 column and in this column, peak symmetry and resolution between impurities 2 and 4 was still inadequate under initial mobile phase conditions. Therefore, the mobile phase was further optimized to include 5 mM ammonium formate buffer (pH adjusted to 4.0), methanol, and acetonitrile in different proportions. The combination of acetonitrile and methanol as organic modifiers enhances the selectivity and peak resolution due to their differential polarity and elution strengths. Further, QbD-based DoE strategy was implemented and this approach allows more targeted and statistically guided optimization of buffer strength and pH. The final optimized method utilizes BEH C18 column (100 mm × 2.1 mm, 1.7 µm) at 35 °C, with isocratic elution using 5 mM ammonium formate/formic acid buffer (pH 3.5), acetonitrile, and methanol in a 45:35:20 (v/v) ratio, at 0.3 mL/min and UV detection at 265 nm. Method validation was results demonstrate excellent specificity, linearity (R^2 > 0.999 for all analytes), precision (RSD < 1 %), accuracy (recovery between 98–102 %), and sensitivity (LOD as 0.075 µg/mL for impurities). The method was also highly selective, with no interferences from placebo or excipients, confirms its suitability for routine impurity profiling of fruquintinib. The stability-indicating nature of the method was established through extensive forced degradation studies and significant degradation was witnessed in acidic and peroxide conditions with multiple DPs. The LC-MS/MS analysis enables characterization of this DP (DP-5), with accurate mass measurement (*m/z* 223.1976) and elucidation of its likely formation via oxidative cleavage of the ether linkage in the fruquintinib structure that leads to a hydroperoxide intermediate. The QbD approach effectively captures the interaction of key parameters and further expansion need to conduct in design space to include temperature and column dimensions. This approach enhances the method transferability across different chromatographic systems. In conclusion, the developed chromatographic method was robust, accurate, and reliable analytical tool for the simultaneous estimation of fruquintinib and its impurities. The method's strength lies in its systematic development using a QbD approach, comprehensive validation, and its proven stability-indicating capability. It is thus well-suited for routine use in quality control laboratories that ensures safety, efficacy, and regulatory compliance of fruquintinib pharmaceutical formulations.

References

1. Y. Zhang, J. Y. Zou, Z. Wang, and Y. Wang, *Cancer. Manag. Res.,* **11**, 7787-7803 (2019). http://doi.org/10.2147/CMAR.S215533.
2. Q. Sun, J. Zhou, Z. Zhang, M. Guo, J. Liang, F. Zhou, J. Long, W. Zhang, F. Yin, H. Cai, H. Yang, W. Zhang, Y. Gu, L. Ni, Y. Sai, Y. Cui, M. Zhang, M. Hong, J. Sun, Z. Yang, W. Qing, W. Su, and Y. Ren, *Cancer. Biol. Ther*., **15**(12), 1635-1645 (2014). http://doi.org/10.4161/15384047.2014.964087
3. S. S. Prasad, B. B. Kasimala, and V. R. Anna, *Rasayan. J. Chem.,* **14** (4), 2183-2190 (2021). http://doi.org/10.31788/RJC.2021.1446426
4. B. B. Kasimala, V. R. Anna, and U. R. Mallu, *Der. Pharmacia. Lett*., **6** (4), 411-419 (2014).
5. S. R. Tummala, K. P. Amgoth. *Turk. J. Pharm. Sci*., **19**(4), 455-461 (2022). https://doi.org/10.4274/tjps.galenos.2021.17702
6. ICH guideline, harmonised tripartite guideline impurities in new drug substances Q3A(R2), 2006.
7. ICH guideline, impurities in new drug products Q3B(R2), 2006.
8. Rajesh Varma Bhupatiraju, Pavani Peddi, Venkata Swamy Tangeti, and Battula Sreenivasa Rao, *Anal. Sci. Technol.,*

37(5), 280-294 (2024). https://doi.org/10.5806/AST.2024.37.5.280

9. Y. B. Mei, S. B. Luo, L. Y. Ye, Q. Zhang, J. Guo, X. J. Qiu, and S. L. Xie, *Drug. Des. Devel. Ther.*, 2865-2871 (2019). https://doi.org/10.2147/DDDT.S199362
10. H. U. Junfeng, Wei Liu, Ying Wang, Xin Chen, Yanwei Guo, Qianqian Peng, Jian Guo, Hongqi Zhang, Shizhong Zhang, and Gaigai Deng, *Biomed. Chromatogr.*, **36**(11), e5459 (2022). https://doi.org/10.1002/bmc.5459
11. Zi-Xuan Guo, Yue-E Wu, Hai-Yan Shi, John van den Anker, Ping Liang, Ying Zheng, Xue-Wei Zhao, Rui Feng, and Wei Zhao, *J. Pharm. Biomed. Anal.,* **224**(5), 115159 (2023). https://doi.org/10.1016/j.jpba.2022.115159
12. B. Rajesh Varma, P. Pavani, T. Venkata Swamy, K. Rekha, and B. Sreenivasa Rao, *Asian. J. Chem.,* **36**(10), 2452-2460 (2024). https://doi.org/10.14233/ajchem.2024.32475
13. K. M. Amgoth, S. R. Tummala, *J. Res. Pharm.*, **26**(6), 1685-1693 (2022). https://doi.org/10.29228/jrp.259
14. Rajesh Varma Bhupatiraju, Pavani Peddi, Subhashini Edla, Kandula Rekha, and Bikshal Babu Kasimala, *Sep. Sci. plus.,* **7**(9), e202400106 (2024). https://doi.org/10.1002/sscp.202400106
15. ICH guideline, stability testing of new drug substances and products Q1A(R2), 2003.
16. S. R. Tummala, N. Gorrepati, H. K. Tatapudi. *Curr. Pharm. Anal.,* **20**(8), 944–952 (2024). https://doi.org/10.2174/0115734129332940240919113159